Intestinal CD103+, but not CX3CR1+, antigen sampling cells migrate in lymph and serve classical dendritic cell functions

Olga Schulz,[1] Elin Jaensson,[2] Emma K. Persson,[2] Xiaosun Liu,[1] Tim Worbs,[1] William W. Agace,[2] and Oliver Pabst[1]

[1]Institute of Immunology, Hannover Medical School, Hannover 30625, Germany
[2]Immunology Section, Lund University, Lund 221 84, Sweden

Chemokine receptor CX3CR1+ dendritic cells (DCs) have been suggested to sample intestinal antigens by extending transepithelial dendrites into the gut lumen. Other studies identified CD103+ DCs in the mucosa, which, through their ability to synthesize retinoic acid (RA), appear to be capable of generating typical signatures of intestinal adaptive immune responses. We report that CD103 and CX3CR1 phenotypically and functionally characterize distinct subsets of lamina propria cells. In contrast to CD103+ DC, CX3CR1+ cells represent a nonmigratory gut-resident population with slow turnover rates and poor responses to FLT-3L and granulocyte/macrophage colony-stimulating factor. Direct visualization of cells in lymph vessels and flow cytometry of mouse intestinal lymph revealed that CD103+ DCs, but not CX3CR1-expressing cells, migrate into the gut draining mesenteric lymph nodes (LNs) under steady-state and inflammatory conditions. Moreover, CX3CR1+ cells displayed poor T cell stimulatory capacity in vitro and in vivo after direct injection of cells into intestinal lymphatics and appeared to be less efficient at generating RA compared with CD103+ DC. These findings indicate that selectively CD103+ DCs serve classical DC functions and initiate adaptive immune responses in local LNs, whereas CX3CR1+ populations might modulate immune responses directly in the mucosa and serve as first line barrier against invading enteropathogens.

CORRESPONDENCE
Oliver Pabst:
Pabst.Oliver@MH-Hannover.de
OR
William W. Agace:
William.Agace@med.lu.se

Abbreviations used: ALDH, aldehyde dehydrogenase; eYFP, enhanced YFP; LP, lamina propria; LPC, LP cell; MLN, mesenteric LN; RA, retinoic acid; TLR, toll-like receptor.

The intestinal mucosa contains large numbers of mononuclear cells, including macrophages and DCs, which together are believed to play a central role in regulating mucosal innate and adaptive immune responses in both the steady-state and inflammatory setting (Kelsall, 2008). Expression of CD11c and CD11b has been used to distinguish DC subsets from macrophages in the intestine. However, separating subsets of mononuclear cells based on CD11c is complicated because this marker is also expressed on tissue macrophages (Hume, 2008). Furthermore, there is currently little evidence to suggest that subdividing mononuclear lamina propria (LP) cells (LPCs) based on CD11c and CD11b defines populations with distinct turnover rates, origins, and functional properties.

Based on the observation that DC can penetrate epithelial monolayers in vitro and a close association of CD11c-expressing cells with the gut epithelium in vivo, Rescigno et al. (2001) put forward the idea of epithelial-associated DC that is capable of capturing luminal bacteria and transporting them into the intestinal LP. Further studies using transgenic mice expressing GFP under the control of the CX3CR1-promoter (CX3CR1$^{+/GFP}$ mice) confirmed that a major subset of mononuclear cells in the intestinal LP are capable of extending processes across the epithelial layer into the intestinal lumen (Niess et al., 2005). In vivo invasion-defective *Salmonella enterica* were associated with CX3CR1-expressing cells in the intestinal LP of transepithelial-proficient, but not transepithelial dendrite-deficient, CX3CR1$^{GFP/GFP}$ mice, suggesting that transepithelial dendrites play an

O. Schulz and E. Jaensson contributed equally to this paper.
W. Agace and O. Pabst contributed equally to this paper.

The Rockefeller University Press $30.00
J. Exp. Med. Vol. 206 No. 13 3101-3114
www.jem.org/cgi/doi/10.1084/jem.20091925

important role in sampling and uptake of luminal microbes (Niess et al., 2005; Hapfelmeier et al., 2008). Such transepithelial dendrites have also been observed in CD11c and MHCII reporter mice (Niess et al., 2005; Chieppa et al., 2006) even though their frequency and distribution remains controversial (Chieppa et al., 2006; Vallon-Eberhard et al., 2006). Together, these studies have led to the prevailing assumption that epithelial-associated CX3CR1$^+$ mononuclear LPCs are DCs that play an important role in the initiation of intestinal adaptive immune response (Rescigno, 2003; Chieppa et al., 2006; Niess and Reinecker, 2006). Nevertheless, definitive evidence that CX3CR1$^+$ LPCs are tissue DCs that are capable of migrating to draining mesenteric LN (MLN) and priming T cell responses has not been provided.

We, and others, have identified a subset of DC in the intestinal LP and MLN which expresses the integrin α chain CD103. These cells display an intrinsic ability to induce the gut-homing receptors CCR9 and α4β7-integrin on responding T cells (Annacker et al., 2005; Johansson-Lindbom et al., 2005) and FoxP3 Treg differentiation in vitro (Coombes et al., 2007; Sun et al., 2007). Both of these functions appear to be caused by an enhanced ability of intestinal CD103$^+$ DC to induce retinoic acid (RA) receptor signaling in responding T cells (Jaensson et al., 2008; Svensson et al., 2008) and are associated with higher expression of the gene encoding RALDH2 (retinaldehyde dehydrogenase 2), *aldh1a2* (Coombes et al., 2007), a key enzyme involved in retinal metabolism. Importantly, CD103$^+$ DCs are also present in human MLN and selectively induce RA receptor–dependent CCR9 expression on allogenic T cells (Jaensson et al., 2008). Thus, expression of CD103 identifies a DC subset that, under the influence of environmental conditioning in the gut and in the MLN (Agace, 2008; Hammerschmidt et al., 2008), confers typical properties of intestinal immune responses. CD103$^+$ DCs are dramatically reduced in the MLN, but not LP, of CCR7$^{-/-}$ mice (Johansson-Lindbom et al., 2005; Worbs et al., 2006) and, in BrdU pulse-chase experiments, have been shown to turn over rapidly in the LP in the steady state and with delayed kinetics in the MLN, suggesting that CD103$^+$ MLN DCs represent LP-derived migratory DCs (Jaensson et al., 2008). Finally, CD103$^+$, but not CD103$^-$, MLN DCs are capable of priming OT-I and OT-II cells ex vivo after oral administration of OVA, indicating that these cells play a central role in initiating T cell responses to soluble luminal antigen (Coombes et al., 2007; Jaensson et al., 2008). Despite these findings, it remains unclear whether intestinal CD103$^+$ DC and CX3CR1$^+$ cells represent phenotypically and functionally overlapping or distinct populations of cells in the intestinal LP.

In this paper, we demonstrate that CD103 and CX3CR1 expression defines distinct LPC populations. Although CD103$^+$ DCs are short lived, travel via intestinal lymph to the gut draining MLN, and efficiently present antigens to naive T cells, CX3CR1$^+$ cells are comparably longer lived LP-resident cells, cannot be observed in intestinal lymph, and are poor at presenting antigen to naive T cells. Together, these results suggest a division of labor between gut-resident CX3CR1$^+$ LPC and migratory antigen-presenting CD103$^+$ DC in the intestinal immune system.

RESULTS

CX3CR1 and CD103 identify nonoverlapping subsets of LP mononuclear cells

Defining LP mononuclear cell subsets based on MHCII, CD11b, and CD11c is complicated because of variations in the expression levels of these markers, resulting in often overlapping and uncertain definitions of cell populations (unpublished data; Chieppa et al., 2006; Uematsu et al., 2006, 2008). Because a prominent subset of LPC, which is capable of extending cellular processes through the gut epithelium, has been described using CX3CR1$^{+/GFP}$ mice (Niess et al., 2005; Vallon-Eberhard et al., 2006), we used CX3CR1$^{+/GFP}$ mice to assess CX3CR1, MHCII, CD11c, and CD103 expression on LPC by confocal microscopy and flow cytometry. Consistent with a putative function in antigen sampling, CX3CR1/GFP$^+$ cells localized close to the intestinal epithelium (Fig. 1 A). In confocal microscopy, CX3CR1/GFP$^+$ LPC showed variable expression of CD11c and no expression of CD103 (Fig. 1 A). In contrast, CD103 was evident as CD11c^{bright} LPC with no detectable expression of CX3CR1/GFP (Fig. 1 A) and these cells preferentially localized in the villus core (Fig. 1 A). Enumeration of CX3CR1/GFP$^+$ and CD103$^+$ CD11c$^+$ LPC revealed roughly three- to fourfold more cells of the former compared with the latter LPC population (Fig. 1 A). These observations suggest that CD103 and CX3CR1/GFP identify nonoverlapping subtypes of small intestinal LPC.

Flow cytometry of isolated LPC confirmed these observations. The CD103$^+$ LPC population comprised a substantial fraction of MHCII$^+$CD11c$^+$ cells that showed very weak CX3CR1/GFP signals (Fig. 1 B and Fig. S1 A). LPC expressing CX3CR1/GFP levels that potentially might be detected by fluorescent microscopy could be divided into two distinct populations distinguished by high and intermediate CX3CR1/GFP expression (Fig. 1 B). Freshly isolated CX3CR1/GFP^{high} LPCs were MHCII$^+$CD11b$^+$. These cells also expressed the macrophage markers CD14 and F4/80 and most expressed CD11c, although at consistently lower levels than CD103$^+$ MHCII$^+$ cells. Based on these markers, CX3CR1/GFP^{high} cells appear to represent a homogenous LPC population (Fig. 1 B and Fig. S1 B). Although the majority of CX3CR1/GFP^{int} LPC also expressed MHCII and CD11b, this population appeared phenotypically more heterogeneous. Although most CX3CR1/GFP^{int} LPC expressed F4/80 and CD14, albeit at lower levels than CX3CR1/GFP^{high} cells, this population also contained a variable proportion of MHCII$^-$ cells that were predominantly GR-1^{hi}CD11b$^+$CD11c CD62L$^+$ CCR2^{high}, a phenotype which is similar to that of circulating inflammatory monocytes (Fig. 1 B, Fig. S1C, and not depicted; Landsman et al., 2007). For brevity, we refer to CD103$^+$MHCII$^+$CD11c$^+$CX3CR1$^-$ LPC as CD103$^+$ DC. Because CX3CR1/GFP-expressing LPCs share phenotypic traits with both macrophages

and DC, we will refer to these cells either as CX3CR1^{high} or CX3CR1^{int} LPC or summarize both populations as CX3CR1^{+} LPC.

CX3CR1^{+} LPC and CD103^{+} DC display distinct turnover rates in the steady state and responsiveness to growth factors

By performing small bowel transplantations, we have recently reported that maintenance of the CD103^{+} DC compartment requires continual influx of precursors from extraintestinal sources (Jaensson et al., 2008). However, in sections from these transplants we noted that CD11c^{+} cells displaying weak MHCII expression showed long-term persistence in grafted intestinal fragments (Fig. 2 A; Jaensson et al., 2008). Because CX3CR1^{+} LPCs show detectable CD11c expression (Fig. 1 A) when analyzed by immunofluorescence microscopy, we speculated that the CD11c^{+} cells that were maintained in the transplants

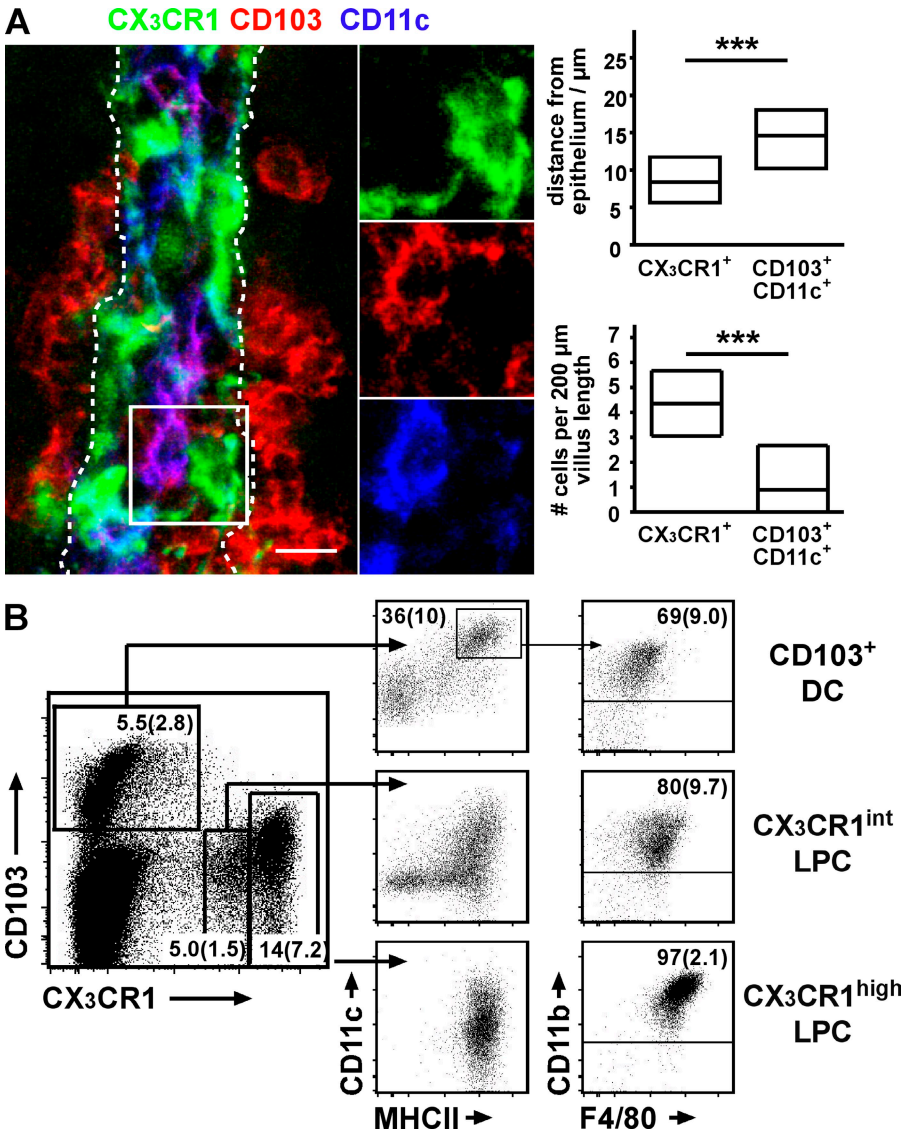

Figure 1. CX3CR1 and CD103 characterize distinct sets of LP mononuclear cells. (A) 50-µm cryosections of CX3CR1$^{+/GFP}$ mice were stained for CD11c and CD103 and analyzed by confocal microscopy. The image shows an orthogonal projection of a 7.5-µm z-stack depicting CX3CR1/GFP (green), CD103 (red), and CD11c (blue). The boxed region is shown in detail in split channels. The dashed lines indicate the epithelial border/basal lamina. Bar, 10 µm. The localization of CX3CR1/GFP^{+} and CD103^{+}CD11c^{+} cells in the proximal ileum with respect to the basal epithelium and their numbers were determined using 7-µm-thick cryosections documented by epifluorescence microscopy. Diagrams depict mean and 25th and 75th percentiles as boxes. Sections obtained from four mice in two independent experiments were evaluated and a total of 116 CD103^{+} and 584 CX3CR1^{+} cells were analyzed. ***, $P < 0.001$. (B) Flow cytometric analysis of CX3CR1$^{+/GFP}$ LPCs. CD103^{+} DCs express very low levels of CX3CR1 and were identified by subgating the CD103^{+}CX3CR1$^{-/low}$ population on CD11c^{+}MHCII^{+} cells. CD11c$^{low/-}$MHCII^{-} cells in this plot are removed when gating on CD3^{-}CD19^{-} cells, suggesting they are T cells (not depicted). CX3CR1^{+} LPCs could be further subgrouped into CX3CR1^{int} and CX3CR1^{high} LPC populations. All three populations were analyzed for expression of CD11b and F4/80. Numbers indicate mean percentage (SD) of cells in the respective gate of 10 mice analyzed in at least four independent experiments. The total percentage of CD103^{+} DC among CD45^{+} cells is 1.9% (SD, 1).

represented CX3CR1^{+} LPC. To assess this possibility, a small intestinal fragment, including the draining MLN, was isolated from CX3CR1/GFP mice and transplanted into syngenic WT recipients. 9 d after transplantation, the frequency of CX3CR1^{+} LPC in the grafted intestinal fragment was determined by immunofluorescence microscopy and compared with non-transplanted CX3CR1/GFP mice. Strikingly, and in marked contrast to CD103^{+} DCs (Jaensson et al., 2008), CX3CR1^{+} LPCs were not reduced in the grafted small intestine compared with unmanipulated CX3CR1$^{+/GFP}$ mice (Fig. 2 B). This indicates that CX3CR1^{+} LPCs are not rapidly replaced from extraintestinal sources, even though surgery might promote loss of cells from the transplanted tissue. To compare the turnover of CX3CR1^{+} LPC and CD103^{+} DC in the steady state, CX3CR1$^{+/GFP}$ mice were injected with a single dose of BrdU. Consistent with our observation that these cells turn over rapidly in vivo (Jaensson et al., 2008), 9 h after injection almost 10% of CD103^{+} DC had incorporated BrdU (Fig. 2 C). In contrast, both CX3CR1^{int} and CX3CR1^{high} LPCs showed significantly lower rates of BrdU incorporation (Fig. 2 C). Finally, to determine the impact of different DC/myeloid cell growth factors on CX3CR1^{+} LPC and CD103^{+} DC compartments in vivo, CX3CR1$^{+/GFP}$ mice were injected with melanoma cells constitutively secreting Flt3L or GM-CSF and, after 6–12 d, the numbers of CX3CR1^{+} LPCs and CD103^{+} DCs were determined by fluorescence microscopy and flow cytometry. CD103^{+} DCs efficiently expanded in mice carrying either Flt3L (Fig. 3, A and B) or GM-CSF–producing tumors (Fig. 3 B). In contrast, CX3CR1^{high} LPC failed to respond to either cytokine, whereas CX3CR1^{int} LPC showed expansion to Flt3L. Collectively, these results demonstrate that CD103^{+} DC and CX3CR1^{+} LPC display different turnover rates and responses to Flt3L and GM-CSF and, thus, likely derive from distinct precursor populations.

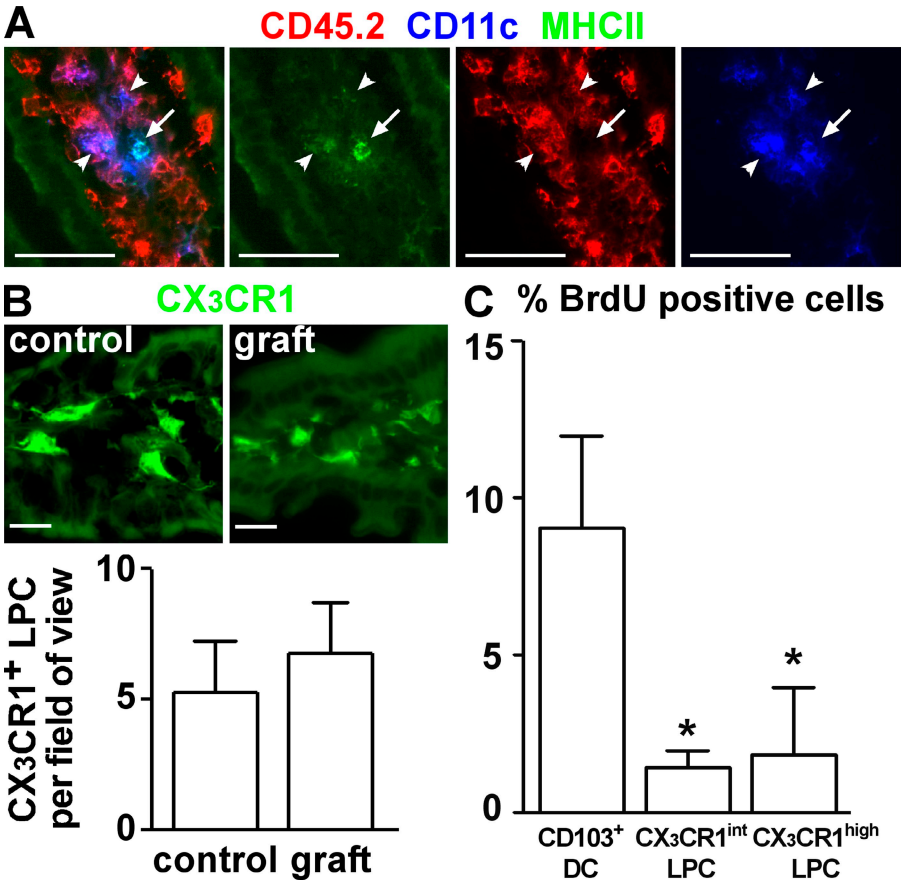

Figure 2. CX3CR1^{+} LPCs, but not CD103^{+} DCs, display long-term persistence in small bowel transplants. (A) CD45.2^{+} intestinal fragments were grafted into CD45.1^{+} recipients and analyzed by fluorescence microscopy. 6 d after transplantation, the majority of CD11c^{+}MHCII^{+} (arrows) cells in the grafted tissue did not express CD45.2, i.e., had been replaced by host cells. In contrast, CD11c^{+} cells with low MHCII signal (arrowheads) were mostly CD45.2^{+}, which is indicative of donor origin and long-term persistence in the grafted tissue. Bars, 50 µm. Six mice were analyzed in six experiments. (B) Intestinal fragments were grafted from CX3CR1$^{+/GFP}$ donors into WT recipients. 9 d after transplantation, the number of CX3CR1/GFP^{+} cells in the grafted tissue was enumerated by epifluorescence microscopy and compared with unmanipulated CX3CR1$^{+/GFP}$ mice (control). Error bars represent SD. Bars, 20 µm. Two mice were analyzed in two experiments. (C) CX3CR1$^{+/GFP}$ mice were injected i.p. with 2 mg BrdU and, 9 h later, the percentage of BrdU-positive CD103^{+} DC and CX3CR1^{+} LPC was determined by flow cytometry. Six mice were analyzed in three independent experiments. Error bars represent SEM. Results were obtained with a Wilcoxon signed rank test. *, $P < 0.05$.

CD103⁺ DCs, but not CX3CR1⁺ LPCs, migrate in intestinal lymph

A paradigmatic view of the DC life cycle is that immature DCs sample antigen in the periphery, mature, and migrate via the lymphatics into the draining LNs to present antigen. We have previously provided indirect evidence that CD103⁺ DCs are a migratory population of cells that continually migrate to the draining MLN (Johansson-Lindbom et al., 2005; Hammerschmidt et al., 2008; Jaensson et al., 2008). To directly determine whether CD11c⁺ DCs and/or CX3CR1⁺ LPCs migrate from the small intestine to the MLN, we performed multiphoton confocal microscopy on

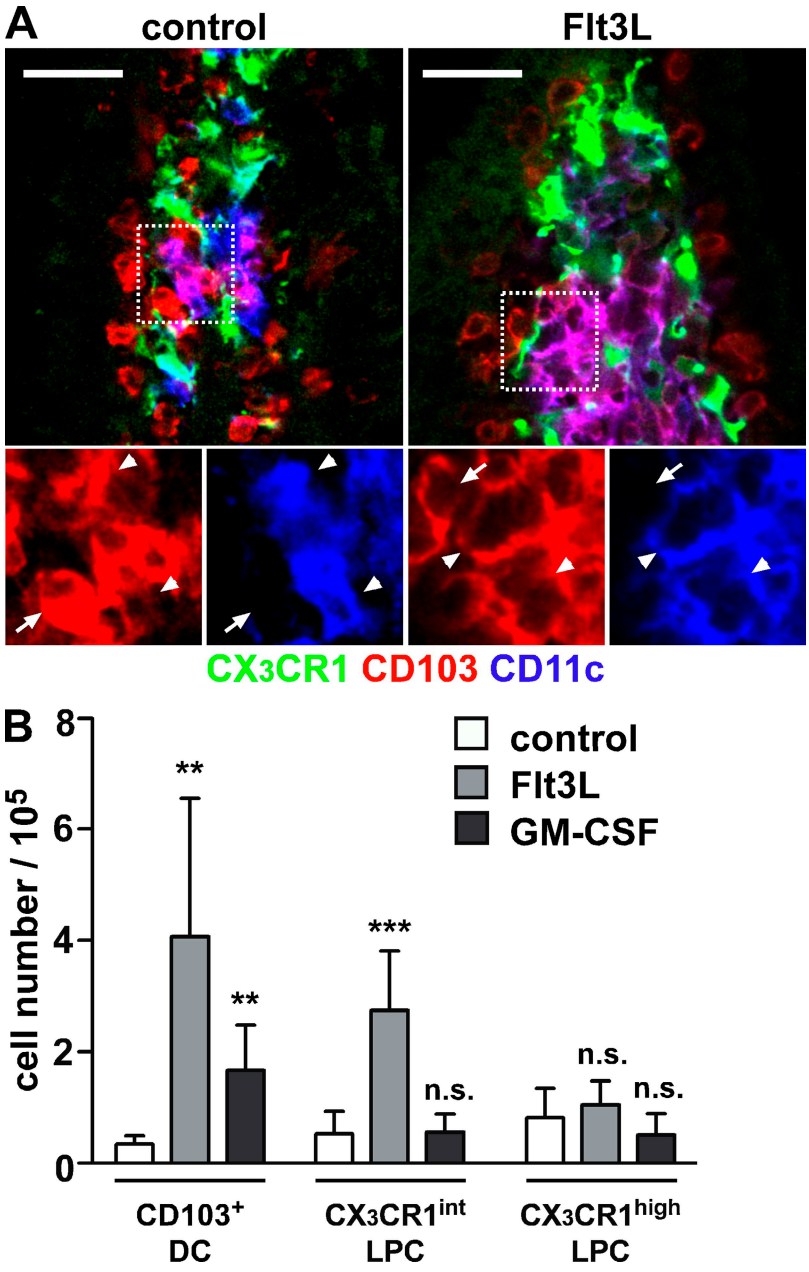

Figure 3. CX3CR1⁺ LPC and CD103⁺ DC display different responsiveness to Flt3L and GM-CSF in vivo. Melanoma cells secreting Flt3L or GM-CSF were injected subcutaneously into CX3CR1$^{+/GFP}$ mice and animals were sacrificed 6–12 d later. (A) 12 d after injection of Flt3L-secreting tumor cells, confocal microscopy revealed massive expansion of intestinal CD103⁺ DC but not CX3CR1⁺ LPC. Images show representative stainings for CX3CR1/GFP (green), CD103 (red), and CD11c (blue). The boxed region in split channels is shown on the bottom. Arrowheads indicate CD11c⁺CD103⁺ LP DC and arrows mark CD11c⁻CD103⁺ cells, most likely representing T cells. Three mice were analyzed in three independent experiments. Bars, 20 µm. (B) The total number of isolated CD103⁺ DC, CX3CR1^{high} LPC, and CX3CR1^{int} LPC in tumor-bearing mice was determined by flow cytometry. Mean (SD) is shown of at least six mice per group analyzed in two (GM-CSF) and three (Flt3L) independent experiments. Results were obtained with an unpaired Student's *t* test. **, $P < 0.01$; ***, $P < 0.001$.

mesenteric lymph vessels. Lymph vessels were readily identified in olive oil–fed mice as whitish vessels running in parallel to mesenteric blood vessels (Fig. 4 A; Hammerschmidt et al., 2008). To facilitate identification of lymph vessels by fluorescence microscopy, we injected fluorescently labeled dextran 30 min before sacrificing the mice. Fluorescently labeled dextran selectively highlights blood vessels shortly after i.v. injection, whereas 30 min after injection, blood and lymph vessels are both labeled (Fig. 4 A). Lymph vessels were readily visible by bright-field microscopy, TRITC fluorescence signal, and a second harmonics signal, visualizing the collagen-rich vessel wall. Cells present in the vessel lumen appeared as dark TRITC-excluding shadows (Fig. 4 B). Using mice expressing enhanced YFP (EYFP) under control of the CD11c promoter (CD11c-EYFP mice), we readily identified CD11c-expressing cells in intestinal lymph

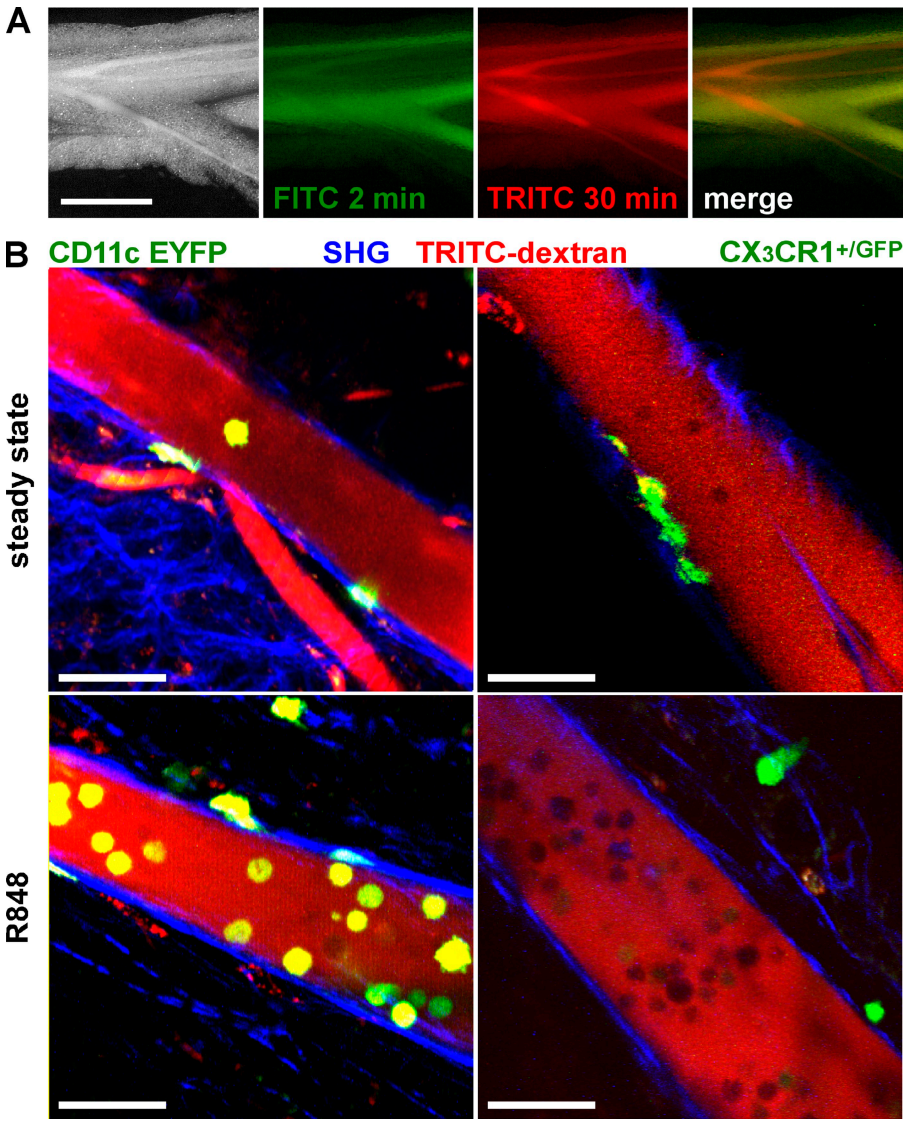

Figure 4. R848 administration mobilizes CD11c/YFP$^+$, but not CX3CR1/GFP$^+$, cells into MLN-afferent lymph. (A) Visualization of MLN-afferent lymphatics. 1 h after gavage of 200 µl of olive oil, lymphatics appear as bright/white vessels running in parallel to mesenteric blood vessels (left). FITC- and TRITC-labeled dextran injected i.v. 2 and 30 min before analysis (green and red, respectively) can differentially highlight blood vessels or both blood vessels and lymphatics. In the merge (right) image, blood vessels appear yellow and lymph vessels red. Bar, 1 mm. (B) Two-photon microscopy of MLN-afferent lymphatics of CD11c-EYFP and CX3CR1$^{+/GFP}$ mice in the steady state or 5 h after oral administration of R848. TRITC-labeled dextran was injected i.v. 30 min before mice were sacrificed to visualize the vessel lumen (red). Collagen-rich vessel walls display a second harmonic signal (blue). The images show orthogonal projections of 20-µm-thick (CD11c-EYFP mice) or 5-µm-thick (CX3CR1/GFP mice) volumes. Bars, 50 µm. CD11c-positive cells were readily detectable in steady-state lymphatics (top left, green) and in increased numbers 5 h after gavage of 10 µg R848 (bottom left). CX3CR1-positive cells typically occurred in the shape of stellate morphology cells on the outside of vessel tubes or within the vessel wall (top right). Cells not expressing the reporter GFP/YFP appeared as TRITC-excluding shadows in the lumen. Pictures shown are from non–Peyer's Patch draining lymphatics. The following numbers of independent experiments were each performed with single mice: CD11c-EYFP, five; CD11c-EYFP$^+$R848, two; CX3CR1$^{+/GFP}$, four; and CX3CR1$^{+/GFP}$R848, five.

vessels (Fig. 4 B, top left). CD11c/YFP$^+$ cells in lymph vessels showed a rounded morphology, and careful analysis of Z-stacks confirmed intraluminal localization as judged by the collagen/SHG signal. CD11c/EYFP-expressing cells were scarce but could be demonstrated in almost all image stacks analyzed (unpublished data). Extending these experiments to CX3CR1$^{+/GFP}$ mice, CX3CR1/GFP-expressing cells were detectable in surrounding fatty tissue, either as scattered cells or in compact cell clusters (not depicted), and occasionally on the extraluminal side of the lymph vessels (Fig. 4 B, top right; and Video 1). This latter population displayed stellate cell morphology and in some cases extended protrusions into the lymph vessel. However, in striking contrast to CD11c/EYFP$^+$ cells, CX3CR1/GFP$^+$ cells were almost undetectable within intestinal lymph vessels (Video 1). Of four mice analyzed, only in one case were a total of four CX3CR1/GFP-expressing cells observed in the lymph vessel lumen.

R848 signaling via Toll-like receptor (TLR) 7/8 enhances the migration of DC from the LP into the MLN (Yrlid et al., 2006). Such R848-induced mobilization of DC is accompanied by a massive increase in serum levels of proinflammatory cytokines and does not depend on direct TLR stimulation on the DC (Yrlid et al., 2006). We thus used oral R848 application to investigate the presence of CD11c- and CX3CR1-expressing cells in intestinal lymph under inflammatory conditions. 5 h after oral administration of R848 to CD11c-EYFP mice, the number of CD11c/EYFP$^+$ cells in intestinal lymph was markedly increased compared with steady-state conditions (Fig. 4 B, bottom left; and Video 2). Oral application of R848 to CX3CR1$^{+/GFP}$ mice, however, failed to mobilize CX3CR1$^+$ cells into intestinal lymph (Fig. 4 B, bottom right). Thus, direct visualization of CD11c- and CX3CR1-expressing cells in intestinal lymph revealed that CD11c$^+$, but not CX3CR1$^+$, cells migrate in intestinal lymph under steady-state as well as under inflammatory conditions.

To further characterize the CD11c$^+$ cells present in intestinal lymph, we established a novel technique, to isolate cells from murine intestinal lymph vessels for flow cytometric analysis. CX3CR1$^{+/GFP}$ mice received olive oil by gavage and, 1 h later, intestinal lymph vessels were carefully cannulated with a fine capillary. By collecting lymph from several vessels in each mouse, this method allowed us to isolate a total volume of ~0.2–0.4 µl of lymph per mouse (unpublished data). In the steady state, no CX3CR1^{high} cells were detectable in intestinal lymph and <2% of all cells were CD11c$^+$ MHCII$^+$ or expressed intermediate levels of CX3CR1/GFP. Because of the low numbers of isolated cells, we were unable to further phenotype these populations. In contrast, 5 h after R848 administration up to 40% of all viable cells were CD11c$^+$MHCII$^+$ cells (Fig. 5 A). Importantly, such cells were not observed in intestinal lymph of chemokine receptor CCR7-deficient mice after R848 administration (Fig. 5 A), which is consistent with a central role of CCR7 for DC migration into draining LNs (Ohl et al., 2004; Johansson-Lindbom et al., 2005; Hintzen et al., 2006; Worbs et al., 2006). Phenotypic analysis of CD11c$^+$ cells demonstrated homogenous expression of CD103 and very weak expression of CX3CR1 and, hence, these cells phenotypically resembled intestinal CD103$^+$ DC. In striking contrast to CD103$^+$ DC, we failed to detect CX3CR1^{high} cells in lymph preparations irrespective of R848 application. Furthermore, the frequency of CX3CR1^{int} cells did not increase upon R848 treatment. Thus, in lymph isolated after R848 treatment <50 cells could be isolated expressing intermediate levels of CX3CR1, <20% (10 cells) of which coexpressed MHCII. Given the virtually complete absence of CX3CR1/GFP cells observed in lymph vessels by microscopy and the close association of CX3CR1$^+$ cells with the lymph wall, it seems likely that these cells are contaminants from surrounding tissue. However we cannot, at this point, rule out that a few CX3CR1^{int} cells expressing CX3CR1 levels too low to be detected by microscopy might enter intestinal lymph. Concomitant with the appearance of CD103$^+$ DC in intestinal lymph, 16 h after oral R848 or i.p. LPS administration there was a marked decrease in CD103$^+$ DC in the intestinal LP and accumulation of these cells in the MLN (Fig. 5 B and not depicted). In contrast, the numbers of CX3CR1^{high} and CX3CR1^{int} cells in the LP and MLN remained unchanged. In particular, no CX3CR1^{high} cells could be observed in MLN irrespective of TLR stimulation. Finally, the inability of CX3CR1$^+$ cells to migrate into lymph correlated with an inability of these cells to up-regulate CCR7 12 h after in vitro stimulation with LPS (Fig. S2).

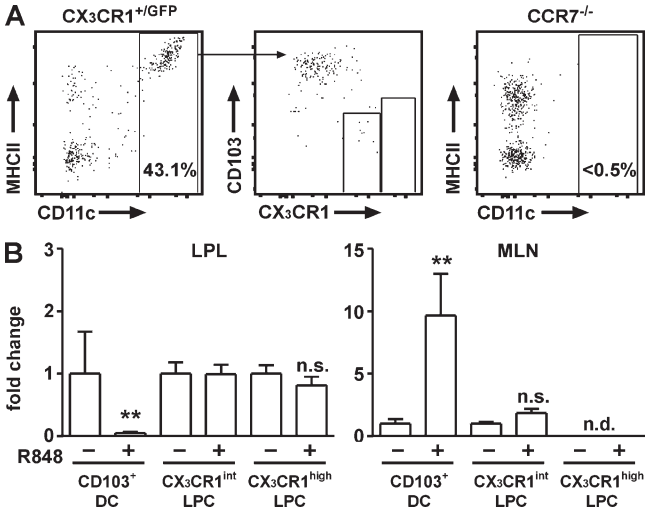

Figure 5. R848 administration mobilizes CD103$^+$ DC, but not CX3CR1$^+$ LPC, into MLN-afferent lymph. (A) Lymph was collected from MLN-afferent vessels 5 h after oral administration of R848 and analyzed by flow cytometry. MHCII$^+$CD11c$^-$ cells express CD19 and, most likely, represent B cells exiting from GALT (not depicted). Results are representative of six experiments. (B) Frequencies of CD103$^+$ DC, CX3CR1^{int} LPC, and CX3CR1^{high} LPC 16 h after oral administration of R848 as determined by flow cytometry. CX3CR1^{high} LPCs were not detected (n.d.) in the MLN. Cell numbers observed in untreated mice were normalized to 1. Bars indicate the according fold change of the mean. Errors bars indicate SD. Four mice per group were analyzed in two independent experiments. Results were obtained with an unpaired Student's *t* test. **, $P < 0.01$.

Collectively, these results demonstrate that, in contrast to CD103$^+$ DCs, CX3CR1$^+$ LPCs are a nonmigratory population of cells in the LP and are thus unlikely to participate in the initiation of adaptive immune responses in intestinal draining LN.

CX3CR1$^+$ LPCs are inefficient at priming naive T cells in vitro and in vivo

Besides their migratory properties, the most distinguishing feature of DCs is their potent antigen-presenting capacity. We therefore isolated CD103$^+$ DC, CX3CR1^{int} LPC, and CX3CR1^{high} LPC and analyzed their ability to present antigen to CD4$^+$ and CD8$^+$ T cells. Isolated cell populations were loaded in vitro with OVA peptide specific for MHC class I–restricted OT-I or MHCII-restricted OT-II T cells. As expected, peptide-loaded CD103$^+$ DC induced efficient proliferation of OT-I and OT-II cells (Fig. 6 A; Johansson-Lindbom et al., 2005). In contrast, CX3CR1^{int} LPC showed a significantly reduced ability to activate OT-I.RAG$^{-/-}$ T cells and, in particular, OT-II.RAG$^{-/-}$ T cells. CX3CR1^{high} LPC induced only very weak proliferation of OT-I.RAG$^{-/-}$ T cells and failed to induce OT-II.RAG$^{-/-}$ or OT-II proliferation (Fig. 6 A and not depicted). Notably, all three LPC populations expressed the costimulatory molecules CD40, CD80, and CD86 (Fig. S3 A). Under steady-state conditions, CD103$^+$ DCs isolated from LP expressed significantly lower levels of CD40 and CD86 compared with CD103$^+$ DCs isolated from the MLN (unpublished data). This situation changed when CD103$^+$ DCs were isolated from the LP after R848 treatment, resulting in increased expression of CD40 and CD86 (Fig. S3 B). However, such up-regulation was less evident on CX3CR1$^+$ LPC (Fig. S3 B), and reduced induction of costimulatory molecules might at least partly explain the low ability of these cells to stimulate T cells.

Because in vitro peptide loading does not recapitulate the entire process of antigen uptake, processing, and presentation, we injected OVA-Cy5 into exteriorized intestinal loops of CX3CR1$^{+/GFP}$ mice to load cells with antigen in vivo. Flow cytometry revealed a higher proportion of antigen-positive CX3CR1$^+$ LPC compared with CD103$^+$ DC, indicating that CX3CR1$^+$ LPC readily took up soluble fluorescently labeled OVA in vivo (Fig. 6 B). Nevertheless, in vivo–loaded CX3CR1$^+$ LPCs were much less efficient in priming OT-II T cells compared with CD103$^+$ DCs (Fig. 6 B). Notably, in CX3CR1$^{GFP/GFP}$ mice, lacking functional CX3CR1 protein, GFP$^+$ LPC also took up fluorescently labeled OVA and adoptively transferred OT-II T cells were activated in the MLN of these mice as efficiently as in WT recipients (Fig. S4, A and B). Because these mice fail to extend transepithelial dendrites (Niess et al., 2005), these results indicate that transepithelial dendrites are dispensable for uptake of and induction of T cell responses to oral soluble antigen.

Compared with the complex situation in an LN, in vitro co-cultures can only recapitulate some aspects of T cell activation. Therefore we investigated the antigen-presenting capacity of CD103$^+$ DC compared with CX3CR1$^+$ LPC in

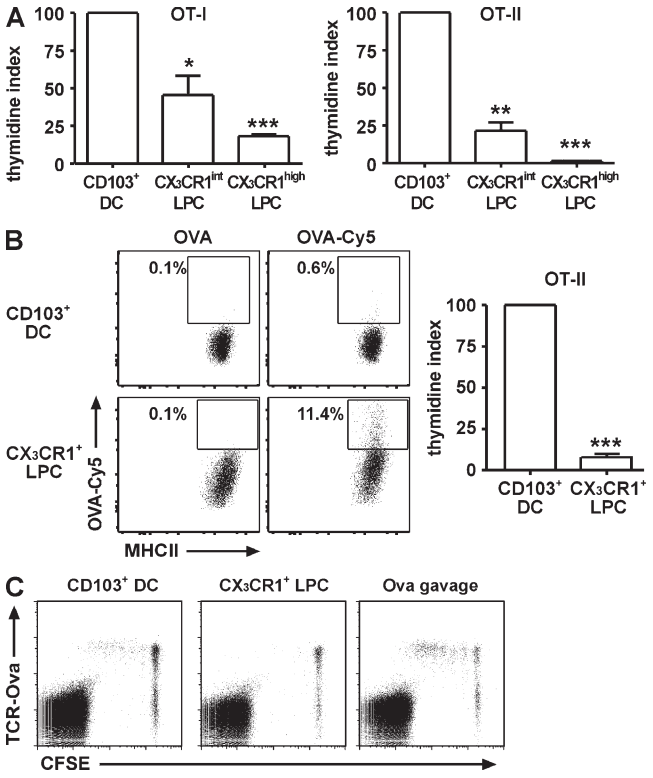

Figure 6. CX3CR1$^+$ LPCs fail to efficiently induce T cell proliferation in vitro and in vivo. (A) OT-I or OT-II cells were co-cultured with peptide-loaded CD103$^+$ DC, CX3CR1^{int} LPC, or CX3CR1^{high} LPC at a ratio of 10:1 for 3 d. Proliferation was determined by thymidine incorporation assay and is depicted as a percentage of the mean T cell proliferation in CD103$^+$ DC co-cultures (thymidine index). Results are the mean (SEM) of three or more independent experiments using pooled cells from four to five mice per experiment. Data were analyzed using one sample Student's *t* test, compared with CD103$^+$ DC. Co-cultures of LPC/T cells at a 1:2 ratio showed a similarly inefficient induction of T cell proliferation compared with the 1:10 ratio (not depicted). *, $P < 0.05$; **, $P < 0.01$; ***, $P < 0.001$. (B) 500 µg of unlabeled or Cy5-labeled OVA was injected into the gut lumen of anaesthetized CX3CR1$^{+/GFP}$ mice. 1 h later, mice were sacrificed and Cy5 fluorescence in CD103$^+$ DC and CX3CR1$^+$ LPC was determined by flow cytometry. Dot plots are gated on CD103$^+$ DC or MHCII$^+$CX3CR1$^+$ LPC as indicated. Gates were adjusted to contain 0.1% of positive cells in controls (injected with unlabeled OVA) and numbers indicate the proportion of Cy5-positive cells. Data are representative of five mice analyzed in three independent experiments. CD103$^+$ DC and CX3CR1^{high} LPC from OVA-Cy5–injected mice were sorted 1 h after injection and co-cultured with OT-II T cells for 3 d at a ratio of 1:10. Cells were pulsed with 1 µCi [^{3}H]thymidine 18 h before collection, and thymidine incorporation was quantified in a β counter. Bars represent pooled data obtained in two independent experiments. Error bars indicate SEM. Results were obtained with a one-sample Student's *t* test. ***, $P < 0.001$. (C) 10^7 CFSE-labeled DO11.10 cells were adoptively transferred to BALB/c recipients. 1 d later, 5,000 peptide-loaded CD103$^+$ DCs or CX3CR1$^+$ LPCs were injected into the MLN-afferent lymphatics. Proliferating antigen-specific T cells were detected in the MLN 3 d after injection. Plots are gated on live CD4$^+$ cells. Control mice received 20 mg OVA by gavage. Results are representative of two independent experiments.

vivo. Sorted CD103$^+$ DC and CX3CR1$^+$ LPC were loaded with OVA peptide specific for MHCII- restricted DO11.10 T cells, and 5,000 antigen-loaded cells were injected into the MLN-afferent lymph of recipient mice that previously received CFSE-labeled DO11.10 cells i.v. 3 d after intralymphatic injection, T cell proliferation was determined in MLN and peripheral LNs. Injection of CD103$^+$ DC induced proliferation of antigen-specific DO11.10 T cells in the MLN but not in peripheral LNs (Fig. 6 C and not depicted). In contrast, antigen-loaded CX3CR1$^+$ LPC failed to induce DO11.10 T cell proliferation in the MLN. Notably, the injected CX3CR1$^+$ LPC included CX3CR1^{high} and CX3CR1^{int} LPC that showed weak but measurable CD4 T cell priming capacity in vitro (Fig. 6 A). Together, these results demonstrate that compared with CD103$^+$ DCs, CX3CR1^{int} LPCs and, in particular, CX3CR1^{high} LPCs have only modest antigen-presenting capacity in vitro and in vivo.

CX3CR1$^+$ LPCs are not imprinted with an enhanced ability to metabolize vitamin A

Given recent studies suggesting an important role for intestinal epithelial cells in imprinting CD11c$^+$ with the ability to metabolize vitamin A and generate gut tropic T cells (Edele et al., 2008; Iliev et al., 2009), and the proximity of CX3CR1$^+$ LPC to the intestinal epithelium, we assessed whether these cells were imprinted with the ability to generate RA. Real-time PCR analysis demonstrated that both CX3CR1^{int} and CX3CR1^{high} LPC expressed significantly lower levels of *aldh1a2* compared with CD103$^+$ DC (Fig. 7 A). To assess whether such differences correlated with differences in aldehyde dehydrogenase (ALDH) activity, CD103$^+$ DC and CX3CR1$^+$ cells were incubated with the fluorescent ALDH substrate ALDEFLUOR, and ALDH activity was assessed by flow cytometry. Because the ALDEFLUOR signal emitted in the FITC channel, we focused on CX3CR1^{high} cells that, in contrast to CX3CR1^{int}, were readily identified in WT mice by gating on F4/80$^+$MHCII^{high}CD11b^{high} cells (Fig. S5). CD103$^+$ DC exhibited significantly higher ALDH activity, compared with CX3CR1^{high} cells, that was blocked with the ALDH inhibitor DEAB (diethylaminobenzaldehyde; Fig. 7, B and C). Finally, to assess whether these differences resulted in a reduced ability of CX3CR1$^+$ LPC to induce CCR9 on responding T cells, CFSE-labeled OT-I cells were incubated together with peptide-pulsed CX3CR1^{high} and CX3CR1^{int} LPCs, and their expression of CCR9 was assessed by flow cytometry. In contrast to CD103$^+$ DC (Fig. 7 D; Johansson-Lindbom et al., 2005; Jaensson et al., 2008), peptide-pulsed CX3CR1^{int} and, in particular, CX3CR1^{high} LPCs were inefficient at inducing CCR9 on responding T cells (Fig. 7 D). Together, these results suggest that CX3CR1$^+$ LPCs are not locally imprinted with an enhanced ability to generate the vitamin A metabolite RA.

DISCUSSION

A paradigm has arisen during the last few years postulating that intestinal LPCs actively sample intestinal antigens through transepithelial dendrites and that such a process might drive the induction of intestinal immune responses in the gut draining MLN. Support for such a model came from numerous studies that, on the one hand, demonstrated transepithelial dendrite-forming cells in live tissue and on the other hand described functional properties of antigen-presenting cells in the LP and draining MLN. However, the interrelation of antigen-sampling cells in the LP and antigen-presenting cells in the MLN has not been directly investigated. Transepithelial dendrite-forming LPCs have mostly been visualized by GFP expressed under control of the CX3CR1 or CD11c promoter (Niess et al., 2005; Chieppa et al., 2006; Vallon-Eberhard et al., 2006), whereas CD103 has been used as a surrogate marker to identify LP-derived DC in the MLN (Annacker et al., 2005; Johansson-Lindbom et al., 2005).

In this study, we used immunofluorescence microscopy and flow cytometry to demonstrate that CD103$^+$ DC and CX3CR1$^+$ LPC represent phenotypically distinct cell populations in the LP. CX3CR1$^+$ LPC outnumbered CD103$^+$ cells three- to fourfold and, in contrast to CD103$^+$ DC, localized close to the epithelium, which is consistent with previous results (Niess et al., 2005; Chieppa et al., 2006). CX3CR1$^+$ LPC could be further divided into CX3CR1^{high} and CX3CR1^{int} LPC populations by flow cytometry. CX3CR1^{high}

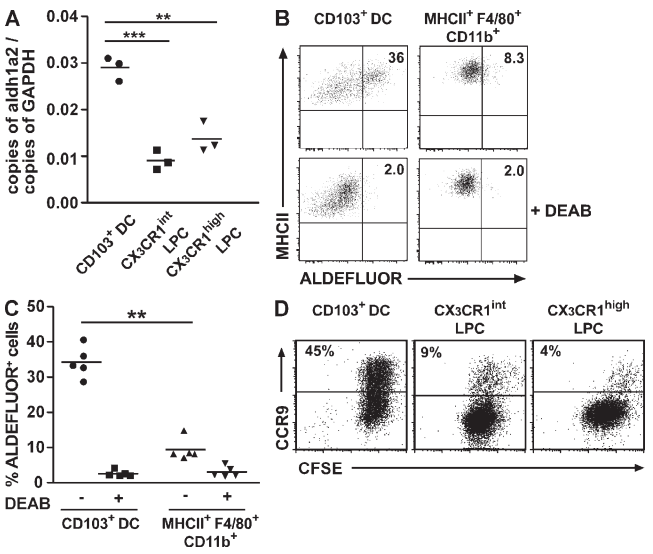

Figure 7. CX3CR1$^+$ LPCs display weak ALDH activity and fail to efficiently induce CCR9 on responding CD8 T cells. (A) *Aldh1a2* expression of sorted CD103$^+$ DC, CX3CR1^{int} LPC, and CX3CR1^{high} LPC was assessed by real-time PCR. The mean (horizontal lines) was obtained from three separate experiments using pooled cells from five to eight mice per experiment. Results were obtained with an unpaired Student's *t* test. **, $P < 0.01$; ***, $P < 0.001$. (B and C) ALDH activity on sorted CD103$^+$ DC and MHCII$^+$F4/80$^+$CD11b$^+$ LPC with or without addition of inhibitor. (B and C) Representative stainings (B) and mean (C; horizontal lines) of five individual mice (symbols). Results were obtained with a paired Student's *t* test. **, $P < 0.01$. (D) CFSE-labeled OT-I cells were co-cultured with peptide-loaded CD103$^+$ DC, CX3CR1^{high} LPC, or CX3CR1^{int} LPC at a ratio of 2:1 for 3.5 d and expression of CCR9 on responding OT-I cells was analyzed. Results are representative of two experiments.

LPCs, which represent the large majority of CX3CR1$^+$ cells in the LP, appeared as a homogenous population of cells expressing CD11b, F4/80, and CD14, markers which are frequently used to identify macrophages. Although most CX3CR1^{int} LPCs also expressed CD11b and F4/80, their variable expression of MHCII, CD11c, and CD14 suggested that this population consisted of several subsets of cells or cells at various stages of maturation.

In addition to their distinct phenotypes, CD103$^+$ DC and CX3CR1$^+$ LPC differed in their responsiveness to growth factors and turnover rates, suggesting that they derive from distinct precursors. CD103$^+$ DC expanded in response to Flt3L and GM-CSF, whereas CX3CR1^{high} LPC failed to expand in response to these cytokines. Moreover, CX3CR1$^+$ cells showed slower turnover rates in vivo and, in contrast to CD103$^+$ DC, were not replaced by recipient cells in small intestinal grafts. These results are consistent with two recent articles that were published while this manuscript was under review (Bogunovic et al., 2009; Varol et al., 2009). Bogunovic et al. (2009) demonstrated an important role for Flt3L and GM-CSF in the generation of CD103$^+$ DC but not CD103$^-$MHCII$^+$CD11c$^+$CD11b$^+$ cells, the large majority of which are CX3CR1$^+$ (unpublished data), and showed that the former cells could derive from pre-DC, whereas the latter derive from Ly6C^{hi} monocytes. Similarly, Varol et al. (2009) demonstrated that Flt3L expanded CD103$^+$CD11b$^-$ DCs, the majority of which likely derive from intestinal isolated lymphoid tissues. However, their findings regarding responsiveness of CD11c$^+$CD11b$^+$ cells to GM-CSF and Flt3L are difficult to interpret, as this population likely includes both CD103$^+$CD11b$^+$ DCs, which make up the majority of CD103$^+$ DCs in the LP, and CD11c$^+$CX3CR1$^+$ LPCs. These authors also demonstrated that CX3CR1^{int} and CX3CR1^{high} cells derived from monocytes, whereas grafted pre-DCs predominantly gave rise to CD11c$^+$CX3CR1$^-$ cells. It is of note that both these studies focused on the fraction of CX3CR1^{high} cells that expressed sufficient levels of CD11c to fall within the CD11c^{high}MHCII^{high} DC gate. However, our current results suggest that these cells are otherwise phenotypically identical to the CD11c$^-$CX3CR1^{high} cells and should not be interpreted to represent classical DCs or a distinct subset of CX3CR1^{high} cells.

Given previous studies suggesting that CX3CR1$^+$ cells capture luminal antigen for initiation of immune responses (Niess et al., 2005; Chieppa et al., 2006; Niess and Reinecker, 2006; Vallon-Eberhard et al., 2006; Hapfelmeier et al., 2008; Uematsu et al., 2008) and indirect evidence indicating that at least a proportion of CD103$^+$ MLN DC derive from the intestinal LP (Johansson-Lindbom et al., 2005; Hammerschmidt et al., 2008), we used two novel technical approaches, multiphoton confocal microscopy of intact lymph vessels and isolation of lymph cells, to determine whether these populations migrated in intestinal lymph. Using these methods, we provide direct evidence to suggest that CD103$^+$ DCs are the dominant migratory DC population in the LP, whereas CX3CR1^{high} LPCs represent a nonmigratory tissue resident population. Using confocal microscopy, no CX3CR1$^+$ cells were observed in lymph under steady-state and inflammatory conditions. In contrast, CD11c$^+$ cells were readily visible and dramatically increased in numbers after R848 administration. Flow cytometry confirmed the absence of CX3CR1^{high} cells in intestinal lymph and revealed that the overwhelming majority of CD11c$^+$MHCII$^+$ cells in lymph were CD103$^+$ and, thus, indistinguishable from CD103$^+$ DC in the LP. Consistently, oral administration of R848 or i.p. administration of LPS (unpublished data) induced a loss of CD103$^+$ DCs from the intestinal LP and a corresponding increase of these cells in the MLN, whereas CX3CR1$^+$ cell numbers remained unchanged. These findings are consistent with studies in LysM-Cre x ROSA26^{flox}stop^{flox}GFP mice, suggesting that the majority of CX3CR1$^+$ cells in the MLN do not derive from the intestinal LP (Bogunovic et al., 2009), and previous studies examining lymph migrating DC in adenectomized rats and pigs (Pugh et al., 1983; Bimczok et al., 2005; Milling et al., 2006), indicating that only a subset of myeloid LPC is capable of entering draining lymph vessels (Bimczok et al., 2005; Yrlid et al., 2006). Moreover, they offer a plausible explanation for the failure in previous studies to observe epithelial-associated CD11c$^+$ cells leaving the LP (Chieppa et al., 2006).

Although we failed to detect CX3CR1$^+$ cells in lymph by confocal microscopy, CX3CR1^{int} cells were detected in low but variable numbers in lymph preparations. We cannot at this point rule out that these few cells derive from the LP; however, CX3CR1$^+$ cells were readily visualized in the fat tissue surrounding the lymph vessels and occasionally had protrusions extending into the lymph vessel. We thus assume that the few CX3CR1^{int} cells in lymph preparations were contaminants from CX3CR1-expressing cells in intimate contact with the vessel wall. Furthermore, the few MHCII$^+$ cells within this population would seem highly unlikely to be in meaningful enough numbers to participate in initiation of T cell responses in the MLN.

To determine whether CX3CR1$^+$ LPC and CD103$^+$ DC displayed direct functional differences in their ability to drive characteristic intestinal T cell responses, we assessed their ability to prime T cell responses in vitro and in vivo. CD103$^+$ DCs were more efficient antigen-presenting cells compared with CX3CR1^{int} and CX3CR1^{high} LPC. Differences in antigen-presenting capacity were generally more pronounced in CD4$^+$ compared with CD8$^+$ T cell priming, in vivo versus in vitro assays, and CD103$^+$ DC compared with CX3CR1^{high} LPC. Moreover, these populations differed in their ability to generate RA, a central signaling molecule involved in shaping the signature of intestinal T cell responses. CX3CR1$^+$ LPCs expressed significantly lower levels of *aldha1a2*, displayed low ALDH activity, and were poor at inducing CCR9 on responding T cells in comparison with CD103$^+$ DC. These latter findings are somewhat surprising given the current dogma that DCs are conditioned by adjacent epithelial cells and recent studies suggesting that intestinal epithelial cells induce *aldha1a2* on bone marrow–derived DCs and imprint them with an ability to induce

gut-homing receptors on responding T cells (Edele et al., 2008; Iliev et al., 2009). A likely explanation for our findings is that epithelial-associated CX3CR1$^+$ LPCs, in contrast to CD103$^+$ DCs, respond poorly to such imprinting signals or that epithelial-derived factors alone are insufficient for such imprinting. It is important to note that our results do not exclude the possibility that intestinal epithelial cells modulate the functionality of LP-resident cell populations, but they suggest that the ability to metabolize retinol is not part of this imprinting program.

An operational definition of a tissue DC should stress the function of DC in transporting antigen and information obtained in peripheral tissues to the draining LNs to activate T cells. Judged by such measure, our results demonstrate that CD103$^+$CD11c$^+$MHCII$^+$ cells fulfil all characteristics of classical tissue DC. In referring to these cells as DCs, it is of relevance to emphasize "their unique life cycle, acting as sentinels in peripheral tissues that on tissue or microbial signals carry self- and foreign antigens to draining lymphoid tissues for the induction of T cell tolerance and immunity" (Kelsall, 2008). In contrast, defining CX3CR1$^+$ LPCs is more problematic because these cells did not migrate in intestinal lymph, displayed weak antigen-presenting capacity in comparison with CD103$^+$ DCs, and share phenotypical traits of both macrophages and DCs.

The question thus arises as to the function of CX3CR1$^+$ LPC in the intestinal mucosa. Numerous publications have examined the antigen-presenting capacity of LP macrophages and DCs and the quality of the ensuing immune response using in vitro co-culture assays (Laouar et al., 2005; Uematsu et al., 2006, 2008; Denning et al., 2007; Atarashi et al., 2008). However, a conclusive synopsis of these findings is complicated because of the divergent strategies used to define distinct subsets of macrophages and DC. The recently described population of intestinal macrophages characterized by CD11b and CD11c appears to largely overlap with CX3CR1^{high} LPC (Denning et al., 2007). These cells have been reported to constitutively produce interleukin 10 and, similarly, we observed intracellular anti–interleukin 10 staining in CX3CR1^{high} LPC (unpublished data). This indicates that constitutive interleukin 10 production by CX3CR1^{high} LPC might contribute to create a tolerance favoring environment in the small intestine.

DCs and macrophages share phenotypical and functional characteristics, and an accentuated point of view might regard DCs as macrophages that display a particular state of activation (Hume, 2008). Along this line, phenotypic descriptions appear to be insufficient to ascertain the nature of myeloid LPCs. In particular, the widely used markers CD11c and CD11b in our hands were unsuitable to distinguish CD103$^+$ migratory DCs and CX3CR1$^+$ gut-resident LPCs (Fig. S1). Moreover, cells expressing typical macrophage markers such as F4/80 have been referred to as DCs or myeloid DC-like cells. Thus, some of the functions assigned to DCs might belong to macrophages and vice versa.

For the future, it will be important to interpret the function of myeloid LPCs based on the anatomical constraints of the intestinal immune system. CX3CR1$^+$ LPCs capable of antigen presentation in vitro are unlikely to encounter naive T cell in vivo because naive T cells are mostly restricted to GALT and MLN and only pass through the LP very infrequently. In this regard, our use of CD103 and CX3CR1 as surrogate markers to define lymph migrating and gut-resident cells is likely to provide an important tool for further dissection of the functionality of LPC subsets.

Although we suggest that CX3CR1$^+$ LPCs do not act as classical DC-priming T cells in draining LN, our data do not rule out a potential role for these cells in modulating the adaptive immune responses. For example, CX3CR1$^+$ LPCs that have been shown to engulf luminal bacteria (Niess et al., 2005; Hapfelmeier et al., 2008) and take up orally administered soluble proteins (this study) may directly pass antigenic material to CD103$^+$ DC still localized in the LP. In this respect, a recent study reported localization of noninvasive *S. enterica* within CX3CR1$^+$ cells in the cecum early after infection, whereas at later time points *S. enterica* were observed within CX3CR1$^-$ cells (Hapfelmeier et al., 2008). Interestingly, uptake of soluble antigen from the intestinal lumen was intact in CX3CR1$^{GFP/GFP}$ mice, indicating that transepithelial extensions would not contribute to sampling of soluble antigen. Moreover, given recent results that antigen-presenting cells drive cytokine and proliferative responses of effector/memory T cells in peripheral tissues (Wakim et al., 2008; McLachlan et al., 2009), antigen presentation by CX3CR1$^+$ LPC may regulate cytokine production and function of antigen-specific effector T cells subsequent to their entry into the intestinal LP. Alternatively, the central role of CX3CR1$^+$ LPC may simply be to serve as a first line of defense by phagocytosing and killing bacteria on the epithelial surface or within the intestinal LP. Consistent with such a function, flagellated *S. enterica* was recently shown to induce MyD88-dependent CX3CR1$^+$ cell migration into the intestinal lumen, suggesting a role for these cells in cell-mediated immune exclusion (Arques et al., 2009).

In summary, our data suggest a division of labor between migrating LP DCs and gut-resident CX3CR1$^+$ cells. CD103$^+$ DCs are capable of intralymphatic migration and enter MLN. In the MLN, cell- and tissue-intrinsic influences, including RA, cooperate to shape the induction of intestinal immune responses. Although future studies are required to determine the potentially diverse in vivo functions of CX3CR1$^+$ LPCs, the realization that these cells represent a gut-resident LP myeloid population will allow more focused efforts toward this goal.

MATERIALS AND METHODS

Mice. B6.129P-CX3CR1^{tm1Litt}/J (Jung et al., 2000; CX3CR1$^{+/GFP}$ mice on C57BL/6 background), BALB/c.129P- CX3CR1^{tm1Litt}/J (CX3CR1$^{GFP/GFP}$ and CX3CR1$^{+/GFP}$ mice on BALB/c background), B6.129P2(C)-Ccr7^{tm1Rfor}/J (CCR7$^{-/-}$ mice [Förster et al., 1999]), C57BL/6-Tg(Tcra Tcrb)1100MjbJ (OT-I mice and OT-I mice crossed to RAG-2–deficient background), C57BL/6-Tg(Tcra Tcrb)425Cbn-Ptprc^a (OT-II Ly5.1 mice and OT-II

mice crossed to RAG-2–deficient background), and BALB/c–Tg(DO11.10) (Do11.10 mice), C57BL/6, BALB/c were bred at the central animal facility of Hannover Medical School and/or Biomedical Center animal facility (Lund University, Lund, Sweden) under specified pathogen-free conditions. CD11c-EYFP (Lindquist et al., 2004) mice were provided by T. Veres (Fraunhofer Institut für Toxikologie und Experimentelle Medizin, Hannover, Germany). All animal experiments were performed in accordance with institutional guidelines and have been approved by the review board of Hannover Medical School and the Niedersaechsische Landesamt für Verbraucherschutz und Lebensmittelsicherheit or by the Lund/Malmö Animal Ethics Committee.

Antibodies and reagents. The following antibodies and reagents were used: CCR9 (7E7; Pabst et al., 2004), CCR2 (MC-21; gift from M. Mack, University of Regensburg, Regensburg, Germany), CD11c-APC (HL3), CD103-PE (M290), CD45.2-PerCP-Cy5.5 (104), CD62L-APC (MEL-14), CD80-PE (16-10A1), CD86-PE (GL1), MHCII($1A^b$)-biotin (AF6-120.1), MHCII($1A^d$)-biotin (AMS-32.1), BrdU-PE (3D4), and rat IgG2b-biotin (G15-337; BD); MHCII(I-A/I-E)-APC (M5/114.15.2) and MHCII(I-A/I-E)–Pacific blue (M5/114.15.2; BioLegend); DO11.10 TCR-bio (KJ1-26; Invitrogen); CCR7-PE (4B12), CD11b-APC-Cy7 (M1/70), CD11c-PE-Cy7 (N418), CD14-APC (Sa2-8), CD103-PE, CD103-biotin (2E7), CD45-PE-Cy7 (30-F11), CD45.2-APC-Cy7 (104), F4/80-APC (BM8), F4/80-PE (BM8), Gr-1-APC (RB6-8C5), Gr-1-PE-Cy7 (RB6-8C5), and Ly6C-biotin (AL-21; eBioscience); and CD40-PE (1C10; Beckman Coulter). APC streptavidin conjugate, Qdot 605 streptavidin conjugate, and streptavidin Alexa Fluor 430 conjugate were obtained from Invitrogen. Dead cells were identified using DAPI staining (Roche), propidium iodine (Invitrogen), 7-amino-actinomycin D (Sigma-Aldrich), or Live Dead Fixable Violet Dead Cell staining kit (Invitrogen). CFSE was obtained from Sigma-Aldrich. Water-soluble R848 was obtained from InvivoGen and LPS (*E. coli* O26:B6) from Sigma-Aldrich. OVA grade III was purchased from Sigma-Aldrich.

Mouse surgery. Small bowel transplantation was performed as described previously (Pabst et al., 2005). 9 d after transplantation, mice were sacrificed and the grafted tissue was embedded for cryosectioning. Injection of OVA into the intestine was performed under the combined anesthesia with Ketamine and Rompun. The small intestine was exposed and 500 µg OVA or Cy5-labeled OVA were injected in 2 vol of 250 µl into the proximal and distal small intestine. The intestine was reintroduced into the body cavity and the skin closed with wound clips. Mice were maintained under anesthesia for 1 h before sacrifice. Intralymphatic injection was performed as previously described (Hammerschmidt et al., 2008).

Cell isolation. For isolation of LPC, Peyer's patches were excised and the intestine was opened longitudinally and incubated 3 × 15 min in HBSS with 10% FCS and 2 mM EDTA at 37°C to remove epithelial cells. After each incubation step, tubes were shaken for 10 s and media containing epithelial cells and debris were discarded. The remaining tissue was incubated for 45 min in RPMI 1640 with 10% FCS, 0.24 mg/ml collagenase A (Roche), and 40 U/ml DNase I (Roche; O. Pabst laboratory) or 0.25 mg/ml collagenase VIII (Sigma-Aldrich) and 50 mM $CaCl_2$ (W.W. Agace laboratory), the tubes shaken for 10 s, and cell suspension collected. This step was repeated one more time and the pooled cell suspension were filtered and either purified by density gradient centrifugation with 40–70% Percoll (GE Healthcare; O. Pabst laboratory) or, alternatively (W.W. Agace laboratory), filtered consecutively through 100- and 40-µm cell strainers (BD). To isolate cells of MLN, LNs were cut into pieces and incubated in the collagenase media described in this section for 45 min and meshed through nylon gaze. Lymph was isolated 1 h after mice received 200 µl of olive oil per gavage to visualize intestinal lymphatics. Mice were sacrificed, lymph was collected with a fine capillary and filtered, and the cellular fraction was washed two times with PBS containing 2% FCS.

Co-culture experiments. For thymidine incorporation assays, $CD103^+$ DCs, $CX3CR1^{int}$ LPCs, and $CX3CR1^{high}$ LPCs were sorted to >95% purity, pulsed with 200 pM OVA 257–264 peptide (Innovagen) or with 560 nM OVA 323–339 peptide (AnaSpec or Innovagen) for 1–2 h at 37°C, washed extensively, and co-cultured with OT-I or OT-II cells, respectively, in round bottom 96-well plates at a ratio of 1:10 (10^4 LPC/10^5 T cells). 1 µCi [^{3}H]thymidine was added after 24 h of co-culture and thymidine incorporation was measured 18 h later. To examine CCR9 induction, OVA 257–264 peptide-pulsed $CD103^+$ DCs, $CX3CR1^{int}$ LPCs, and $CX3CR1^{high}$ LPCs were co-cultured with CFSE-labeled OT-I cells at a ratio of 1:2 (5 × 10^4 LPC/10^5 T cells) and CCR9 expression was assessed by flow cytometry after 3.5 d.

Cell transfer. 10^7 CFSE-labeled DO11.10 cells were adoptively transferred to BALB/c or $CX3CR1^{GPF/GPF}$ BALB/c mice. All mice received a single dose of 50 mg OVA grade III per gavage 4 h after transfer. Proliferation of transferred cells was analyzed on day 3.

Flt3L or GM-CSF–secreting B16 melanoma cells (Mach et al., 2000; provided by N. Mach, Geneva University Hospital, Geneva, Switzerland) were cultured in RPMI 1640 supplemented with 10% FCS, glutamine, and penicillin/streptomycin. Cells were washed thoroughly in PBS before transfer. 5 × 10^6–10^7 cells were injected subcutaneously into each dorsal flank of the mice. Mice were sacrificed after 6–12 d and analyzed by histology and/or flow cytometry.

Flow cytometry. Flow cytometry was performed according to standard procedures. To assess BrdU incorporation, $CX3CR1^{+/GFP}$ mice received an i.p. injection of BrdU (2 mg per mouse; Sigma-Aldrich) and were sacrificed after 9 h. Isolated LPCs were stained with surface antibodies to CD11c, MHCII, CD45.2 and CD103. Live cells were identified using the Live Dead Fixable Violet Dead Cell stain kit (Invitrogen) according to the manufacturer's instructions. Finally, cells were stained with PE-conjugated anti-BrdU antibody (PE BrdU Flow kit; BD) and analyzed on a FACSAria (BD). ALDH activity of $CD103^+$ LP DC and $CX3CR1^{hi}$ LPC was determined using the ALDEFLOUR staining kit (STEMCELL Technologies Inc.) according to the manufacturer's instructions. LPCs were suspended at 10^6 cells/ml in ALDEFLUOR assay buffer containing activated ALDEFLUOR substrate (final concentration 1.5 µM) with or without the ALDH inhibitor DEAB (final concentration 15 µM) and incubated at 37°C for 30 min. ALDEFLUOR-reactive cells were detected in the FITC channel using a FACSAria. Propidium iodide was used to exclude dead cells.

Histological analysis. Intestinal tissue was fixed with cold paraformaldehyde (1% in PBS, pH 7.4) for 3 h and frozen in O.C.T. (Sakura). Cryosections of 7- or 50-µm thickness were stained with anti–CD11c-APC (HL3) and anti–CD103-PE (M290) diluted in TBS with 0.01% Tween at room temperature. Staining was documented using epifluorescence (BX61; Olympus) or confocal laser-scanning (Meta; Carl Zeiss, Inc.) microscopy. Analysis D (Soft Imaging System) software was used to determine the location and frequency of LPCs. Z-stacks obtained by confocal laser-scanning microscopy were combined to volumes using Imaris (Bitplane).

Two-photon microscopy. Mice received 200 µl of olive oil per gavage (1 h before sacrifice) and 400 µg of TRITC-labeled dextran i.v. (MW 70,000; Invitrogen; 30 min before sacrifice) to help the identification of lymphatics. Lymphatics were ligated with suture close to MLN under anesthesia with Ketamine/Rompun. Mice were sacrificed and a 5–8-cm-long intestinal segment corresponding to distal jejunum and proximal ileum with its intact connecting vessels and the MLN was dissected, glued into a cell culture dish, and submerged in cold PBS during the image acquisition to minimize peristaltic movement. Imaging was done on a TriM Scope (LaVision Biotec) equipped with an upright microscope (BX51; Olympus) fitted with a 20× 0.95 NA water immersion objective and a MaiTai Ti:sapphire-pulsed laser (Spectra-Physics) tuned to 865 nm. Image stacks were combined to volumes using Imaris version 6.3.1 and the location of cells was analyzed using the orthoslicer function in XY and XZ direction. Orthogonal projections in Fig. 4 B were generated using two parallel clipping planes (steady-state CD11c-EYFP) or the orthoslicer function in XY direction with extended section (remaining images) to visualize the central 5–20 µm of a vessel.

Real-time PCR. Total RNA was isolated from LPC subsets using RNeasy Micro kit (QIAGEN) and complementary DNA was generated using Superscript III First-Strand kit (Invitrogen) with random hexamers. Expression of *GAPDH* and *aldh1a2* was analyzed using the MyiQ Single-Color Real-Time PCR Detection System (Bio-Rad Laboratories), the Maxima SYBR Green qPCR kit (Fermentas), and the following primers: *GAPDH* forward, 5′-CCTGCACCACCAACTGCTTA-3′; *GAPDH* reverse, 5′-TCATACTTGGCAGGTTTCTCCA-3′; *aldh1a2* forward, 5′-CAGATGCTGACTTGGACTAC-3′; and *aldh1a2* reverse, 5′-ATAAGCTCCAGGACTTTGTT-3′.

Statistical analysis. Statistical analysis was performed with Prism software (GraphPad Software, Inc.) using an unpaired two-tailed Student's *t* test, a paired two-tailed Student's *t* test, a one-sample Student's *t* test, or a Wilcoxon signed rank test as indicated. Error bars represent SD or SEM as indicated. Statistical differences for the mean values are indicated as follows: *, $P < 0.05$; **, $P < 0.01$; ***, $P < 0.001$.

Online supplemental material. Fig. S1 demonstrates the phenotype of CD103$^+$ DC and CX3CR1$^+$ LPC under steady-state conditions. Fig. S2 shows expression of CCR7 on CD103$^+$ DC and CX3CR1$^+$ LPC after LPS stimulation. Fig. S3 shows expression of costimulatory molecules on CD103$^+$ DC and CX3CR1$^+$ LPC under steady-state conditions and after R848 stimulation. Fig. S4 compares uptake of soluble OVA and activation of T cells in WT to CX3CR1$^{GFP/GFP}$ mice. Fig. S5 illustrates gating of CX3CR1$^+$ LPC independent of CX3CR1/GFP reporter activity. Videos 1 and 2 illustrate occurrence of CX3CR1/GFP cells and CD11c/EYFP cells in intestinal lymph vessel in steady state and after R848 stimulation, respectively. Online supplemental material is available at http://www.jem.org/cgi/content/full/jem.20091925/DC1.

We thank Drs. A. Mowat (Glasgow University), B. Johansson-Lindbom (Lund University), R. Förster, and G. Bernhardt (both Hannover Medical School) for invaluable comments on the manuscript and support, Tibor Veres (ITEM, Hannover) for providing CD11c-YFP mice, and Anne-Charlotte Selberg for help with animal care.

This work was supported by grants to W.W. Agace from the Swedish Medical Research Council, the Crafoordska, Österlund, Nanna Svartz and Kocks foundations, the Royal Physiographic Society, the Wellcome Trust, UK and the Swedish foundation for Strategic Research FFL-II program, Deutsche Forschungsgemeinschaft SFB621-TPA11 to O. Pabst, and Excellence Cluster REBIRTH. O. Schulz was supported by a scholarship from Hannover Biomedical Research School.

The authors have no conflicting financial interests.

Submitted: 3 September 2009
Accepted: 12 November 2009

REFERENCES

Agace, W.W. 2008. T-cell recruitment to the intestinal mucosa. *Trends Immunol.* 29:514–522. doi:10.1016/j.it.2008.08.003

Annacker, O., J.L. Coombes, V. Malmstrom, H.H. Uhlig, T. Bourne, B. Johansson-Lindbom, W.W. Agace, C.M. Parker, and F. Powrie. 2005. Essential role for CD103 in the T cell-mediated regulation of experimental colitis. *J. Exp. Med.* 202:1051–1061. doi:10.1084/jem.20040662

Arques, J.L., I. Hautefort, K. Ivory, E. Bertelli, M. Regoli, S. Clare, J.C. Hinton, and C. Nicoletti. 2009. *Salmonella* induces flagellin- and MyD88-dependent migration of bacteria-capturing dendritic cells into the gut lumen. *Gastroenterology.* 137:579–587: 587: e1–e2. doi:10.1053/j.gastro.2009.04.010

Atarashi, K., J. Nishimura, T. Shima, Y. Umesaki, M. Yamamoto, M. Onoue, H. Yagita, N. Ishii, R. Evans, K. Honda, and K. Takeda. 2008. ATP drives lamina propria T(H)17 cell differentiation. *Nature.* 455:808–812. doi:10.1038/nature07240

Bimczok, D., E.N. Sowa, H. Faber-Zuschratter, R. Pabst, and H.J. Rothkötter. 2005. Site-specific expression of CD11b and SIRPalpha (CD172a) on dendritic cells: implications for their migration patterns in the gut immune system. *Eur. J. Immunol.* 35:1418–1427. doi:10.1002/eji.200425726

Bogunovic, M., F. Ginhoux, J. Helft, L. Shang, D. Hashimoto, M. Greter, K. Liu, C. Jakubzick, M.A. Ingersoll, M. Leboeuf, et al. 2009. Origin of the lamina propria dendritic cell network. *Immunity.* 31:513–525. doi:10.1016/j.immuni.2009.08.010

Chieppa, M., M. Rescigno, A.Y. Huang, and R.N. Germain. 2006. Dynamic imaging of dendritic cell extension into the small bowel lumen in response to epithelial cell TLR engagement. *J. Exp. Med.* 203:2841–2852. doi:10.1084/jem.20061884

Coombes, J.L., K.R. Siddiqui, C.V. Arancibia-Cárcamo, J. Hall, C.M. Sun, Y. Belkaid, and F. Powrie. 2007. A functionally specialized population of mucosal CD103$^+$ DCs induces Foxp3$^+$ regulatory T cells via a TGF-β and retinoic acid-dependent mechanism. *J. Exp. Med.* 204:1757–1764. doi:10.1084/jem.20070590

Denning, T.L., Y.C. Wang, S.R. Patel, I.R. Williams, and B. Pulendran. 2007. Lamina propria macrophages and dendritic cells differentially induce regulatory and interleukin 17-producing T cell responses. *Nat. Immunol.* 8:1086–1094. doi:10.1038/ni1511

Edele, F., R. Molenaar, D. Gütle, J.C. Dudda, T. Jakob, B. Homey, R. Mebius, M. Hornef, and S.F. Martin. 2008. Cutting edge: instructive role of peripheral tissue cells in the imprinting of T cell homing receptor patterns. *J. Immunol.* 181:3745–3749.

Förster, R., A. Schubel, D. Breitfeld, E. Kremmer, I. Renner-Müller, E. Wolf, and M. Lipp. 1999. CCR7 coordinates the primary immune response by establishing functional microenvironments in secondary lymphoid organs. *Cell.* 99:23–33. doi:10.1016/S0092-8674(00)80059-8

Hammerschmidt, S.I., M. Ahrendt, U. Bode, B. Wahl, E. Kremmer, R. Förster, and O. Pabst. 2008. Stromal mesenteric lymph node cells are essential for the generation of gut-homing T cells in vivo. *J. Exp. Med.* 205:2483–2490. doi:10.1084/jem.20080039

Hapfelmeier, S., A.J. Müller, B. Stecher, P. Kaiser, M. Barthel, K. Endt, M. Eberhard, R. Robbiani, C.A. Jacobi, M. Heikenwalder, et al. 2008. Microbe sampling by mucosal dendritic cells is a discrete, MyD88-independent step in DeltainvG *S. Typhimurium* colitis. *J. Exp. Med.* 205:437–450. doi:10.1084/jem.20070633

Hintzen, G., L. Ohl, M.L. del Rio, J.I. Rodriguez-Barbosa, O. Pabst, J.R. Kocks, J. Krege, S. Hardtke, and R. Förster. 2006. Induction of tolerance to innocuous inhaled antigen relies on a CCR7-dependent dendritic cell-mediated antigen transport to the bronchial lymph node. *J. Immunol.* 177:7346–7354.

Hume, D.A. 2008. Macrophages as APC and the dendritic cell myth. *J. Immunol.* 181:5829–5835.

Iliev, I.D., E. Mileti, G. Matteoli, M. Chieppa, and M. Rescigno. 2009. Intestinal epithelial cells promote colitis-protective regulatory T-cell differentiation through dendritic cell conditioning. *Mucosal Immunol.* 2:340–350. doi:10.1038/mi.2009.13

Jaensson, E., H. Uronen-Hansson, O. Pabst, B. Eksteen, J. Tian, J.L. Coombes, P.L. Berg, T. Davidsson, F. Powrie, B. Johansson-Lindbom, and W.W. Agace. 2008. Small intestinal CD103$^+$ dendritic cells display unique functional properties that are conserved between mice and humans. *J. Exp. Med.* 205:2139–2149. doi:10.1084/jem.20080414

Johansson-Lindbom, B., M. Svensson, O. Pabst, C. Palmqvist, G. Marquez, R. Förster, and W.W. Agace. 2005. Functional specialization of gut CD103$^+$ dendritic cells in the regulation of tissue-selective T cell homing. *J. Exp. Med.* 202:1063–1073. doi:10.1084/jem.20051100

Jung, S., J. Aliberti, P. Graemmel, M.J. Sunshine, G.W. Kreutzberg, A. Sher, and D.R. Littman. 2000. Analysis of fractalkine receptor CX(3)CR1 function by targeted deletion and green fluorescent protein reporter gene insertion. *Mol. Cell. Biol.* 20:4106–4114. doi:10.1128/MCB.20.11.4106-4114.2000

Kelsall, B. 2008. Recent progress in understanding the phenotype and function of intestinal dendritic cells and macrophages. *Mucosal Immunol.* 1:460–469. doi:10.1038/mi.2008.61

Landsman, L., C. Varol, and S. Jung. 2007. Distinct differentiation potential of blood monocyte subsets in the lung. *J. Immunol.* 178:2000–2007.

Laouar, A., V. Haridas, D. Vargas, X. Zhinan, D. Chaplin, R.A. van Lier, and N. Manjunath. 2005. CD70+ antigen-presenting cells control the proliferation and differentiation of T cells in the intestinal mucosa. *Nat. Immunol.* 6:698–706. doi:10.1038/ni1212

Lindquist, R.L., G. Shakhar, D. Dudziak, H. Wardemann, T. Eisenreich, M.L. Dustin, and M.C. Nussenzweig. 2004. Visualizing dendritic cell networks in vivo. *Nat. Immunol.* 5:1243–1250. doi:10.1038/ni1139

Mach, N., S. Gillessen, S.B. Wilson, C. Sheehan, M. Mihm, and G. Dranoff. 2000. Differences in dendritic cells stimulated in vivo by tumors engineered to secrete granulocyte-macrophage colony-stimulating factor or Flt3-ligand. *Cancer Res.* 60:3239–3246.

McLachlan, J.B., D.M. Catron, J.J. Moon, and M.K. Jenkins. 2009. Dendritic cell antigen presentation drives simultaneous cytokine production by effector and regulatory T cells in inflamed skin. *Immunity*. 30:277–288. doi:10.1016/j.immuni.2008.11.013

Milling, S.W., C. Jenkins, and G. MacPherson. 2006. Collection of lymph-borne dendritic cells in the rat. *Nat. Protoc.* 1:2263–2270. doi:10.1038/nprot.2006.315

Niess, J.H., and H.C. Reinecker. 2006. Dendritic cells in the recognition of intestinal microbiota. *Cell. Microbiol.* 8:558–564. doi:10.1111/j.1462-5822.2006.00694.x

Niess, J.H., S. Brand, X. Gu, L. Landsman, S. Jung, B.A. McCormick, J.M. Vyas, M. Boes, H.L. Ploegh, J.G. Fox, et al. 2005. CX3CR1-mediated dendritic cell access to the intestinal lumen and bacterial clearance. *Science*. 307:254–258. doi:10.1126/science.1102901

Ohl, L., M. Mohaupt, N. Czeloth, G. Hintzen, Z. Kiafard, J. Zwirner, T. Blankenstein, G. Henning, and R. Förster. 2004. CCR7 governs skin dendritic cell migration under inflammatory and steady-state conditions. *Immunity*. 21:279–288. doi:10.1016/j.immuni.2004.06.014

Pabst, O., L. Ohl, M. Wendland, M.A. Wurbel, E. Kremmer, B. Malissen, and R. Förster. 2004. Chemokine receptor CCR9 contributes to the localization of plasma cells to the small intestine. *J. Exp. Med.* 199:411–416. doi:10.1084/jem.20030996

Pabst, O., H. Herbrand, T. Worbs, M. Friedrichsen, S. Yan, M.W. Hoffmann, H. Körner, G. Bernhardt, R. Pabst, and R. Förster. 2005. Cryptopatches and isolated lymphoid follicles: dynamic lymphoid tissues dispensable for the generation of intraepithelial lymphocytes. *Eur. J. Immunol.* 35:98–107. doi:10.1002/eji.200425432

Pugh, C.W., G.G. MacPherson, and H.W. Steer. 1983. Characterization of nonlymphoid cells derived from rat peripheral lymph. *J. Exp. Med.* 157:1758–1779. doi:10.1084/jem.157.6.1758

Rescigno, M. 2003. Identification of a new mechanism for bacterial uptake at mucosal surfaces, which is mediated by dendritic cells. *Pathol. Biol. (Paris).* 51:69–70.

Rescigno, M., M. Urbano, B. Valzasina, M. Francolini, G. Rotta, R. Bonasio, F. Granucci, J.P. Kraehenbuhl, and P. Ricciardi-Castagnoli. 2001. Dendritic cells express tight junction proteins and penetrate gut epithelial monolayers to sample bacteria. *Nat. Immunol.* 2:361–367. doi:10.1038/86373

Sun, C.M., J.A. Hall, R.B. Blank, N. Bouladoux, M. Oukka, J.R. Mora, and Y. Belkaid. 2007. Small intestine lamina propria dendritic cells promote de novo generation of Foxp3 T reg cells via retinoic acid. *J. Exp. Med.* 204:1775–1785. doi:10.1084/jem.20070602

Svensson, M., B. Johansson-Lindbom, F. Zapata, E. Jaensson, L.M. Austenaa, R. Blomhoff, and W.W. Agace. 2008. Retinoic acid receptor signaling levels and antigen dose regulate gut homing receptor expression on CD8+ T cells. *Mucosal Immunol.* 1:38–48. doi:10.1038/mi.2007.4

Uematsu, S., M.H. Jang, N. Chevrier, Z. Guo, Y. Kumagai, M. Yamamoto, H. Kato, N. Sougawa, H. Matsui, H. Kuwata, et al. 2006. Detection of pathogenic intestinal bacteria by Toll-like receptor 5 on intestinal CD11c+ lamina propria cells. *Nat. Immunol.* 7:868–874. doi:10.1038/ni1362

Uematsu, S., K. Fujimoto, M.H. Jang, B.G. Yang, Y.J. Jung, M. Nishiyama, S. Sato, T. Tsujimura, M. Yamamoto, Y. Yokota, et al. 2008. Regulation of humoral and cellular gut immunity by lamina propria dendritic cells expressing Toll-like receptor 5. *Nat. Immunol.* 9:769–776. doi:10.1038/ni.1622

Vallon-Eberhard, A., L. Landsman, N. Yogev, B. Verrier, and S. Jung. 2006. Transepithelial pathogen uptake into the small intestinal lamina propria. *J. Immunol.* 176:2465–2469.

Varol, C., A. Vallon-Eberhard, E. Elinav, T. Aychek, Y. Shapira, H. Luche, H.J. Fehling, W.D. Hardt, G. Shakhar, and S. Jung. 2009. Intestinal lamina propria dendritic cell subsets have different origin and functions. *Immunity*. 31:502–512. doi:10.1016/j.immuni.2009.06.025

Wakim, L.M., J. Waithman, N. van Rooijen, W.R. Heath, and F.R. Carbone. 2008. Dendritic cell-induced memory T cell activation in nonlymphoid tissues. *Science*. 319:198–202. doi:10.1126/science.1151869

Worbs, T., U. Bode, S. Yan, M.W. Hoffmann, G. Hintzen, G. Bernhardt, R. Förster, and O. Pabst. 2006. Oral tolerance originates in the intestinal immune system and relies on antigen carriage by dendritic cells. *J. Exp. Med.* 203:519–527. doi:10.1084/jem.20052016

Yrlid, U., V. Cerovic, S. Milling, C.D. Jenkins, L.S. Klavinskis, and G.G. MacPherson. 2006. A distinct subset of intestinal dendritic cells responds selectively to oral TLR7/8 stimulation. *Eur. J. Immunol.* 36:2639–2648. doi:10.1002/eji.200636426